2014 IEEE International Conference on Robotics & Automation (ICRA)
Hong Kong Convention and Exhibition Center
May 31 - June 7, 2014. Hong Kong, China

Statistical Analysis of Stochastic Multi-Robot Boundary Coverage

Ganesh P. Kumar[1] and Spring Berman[2]

***Abstract*— We present a novel analytical approach to computing the population and geometric parameters of a multi-robot system that will provably produce specified boundary coverage statistics. We consider scenarios in which robots with no global position information, communication, or prior environmental data have arrived at uniformly random locations along a simple closed or open boundary. This type of scenario can arise in a variety of multi-robot tasks, including surveillance, collective transport, disaster response, and therapeutic and imaging applications in nanomedicine. We derive the probability that a given point robot configuration is *saturated*, meaning that all pairs of adjacent robots are no farther apart than a specified distance. This derivation relies on a geometric interpretation of the saturation probability and an application of the Inclusion-Exclusion Principle, and it is easily extended to finite-sized robots. In the process, we obtain formulas for (a) an integral that is in general computationally expensive to compute directly, and (b) the volume of the intersection of a regular simplex with a hypercube. In addition, we use results from order statistics to compute the probability distributions of the robot positions along the boundary and the distances between adjacent robots. We validate our derivations of these probability distributions and the saturation probability using Monte Carlo simulations of scenarios with both point robots and finite-sized robots.**

I. Introduction

Multi-robot systems comprised of large numbers of inexpensive, relatively expendable platforms have the potential to perform tasks on large spatial and temporal scales quickly, robustly, and with little to no human supervision. The production and deployment of such collectives is approaching feasibility due to recent advances in computing, sensing, actuation, power, control, and 3D printing. In the last few years, the miniaturization of these technologies has led to many novel platforms for multi-robot applications, including micro aerial vehicles and nano air vehicles [1], [2] for tasks such as exploration, mapping, environmental monitoring, surveillance, and reconnaissance. At even smaller scales, micro-nano systems are currently being developed for micro object manipulation and biomedical applications, including molecular imaging, drug and gene delivery, therapeutics, and diagnostics [3], [4]. It is now possible to design nanoparticles, DNA machines, synthetic bacteria, and magnetic materials that can move, sense, and interact in a controlled fashion, similar to robotic platforms [5]. These nanorobots will need to be deployed in massive numbers; for instance, trillions of nanoparticles would be required to deliver drugs to a tumor or yield a visible signal for sensing [6].

Many multi-robot applications will involve a *boundary coverage* task, in which robots must arrange themselves along the boundary of a region or object according to a specified density. Possible applications include cooperative manipulation and transport of payloads, surveillance tasks such as perimeter patrolling, and disaster response tasks such as cordoning off a hazardous area or extinguishing a fire. In nanomedicine, therapeutic and imaging applications will require the use of ligand-coated nanoparticles that can bind selectively to cell surfaces with high receptor densities [7].

This paper addresses boundary coverage tasks in which the robots have extremely limited capabilities, as in micro-nanorobotic applications, or in which it is impractical or impossible to use GPS, communication, or prior environmental data, for instance in disaster response operations and intelligence-surveillance-reconnaissance missions. In addition, the boundary coverage task must be accomplished through *stochastic* robot behaviors, which arise from noise due to sensor and actuator errors; randomness in robot encounters with the boundary; and, for nanorobots, the effects of Brownian motion and chemical interactions [3]. There is a sizable body of work on designing stochastic robot control policies that produce different types of desired collective behaviors in multi-robot systems, including assembly and self-assembly [8], [9], [10], [11] and task allocation based on spontaneous robot decisions [12], [13], [14], [15]. Encounter-dependent task allocation strategies are most closely related to our stochastic coverage problem, but existing work either deals with scenarios where encountered objects are small (on the scale of the robot) [16], [17] or where large objects are covered dynamically by the robots [18]. In contrast to previous work, we address a *static* stochastic coverage scenario in which the encountered object or region is *large* compared to the robots.

This paper presents an analytical framework for computing the *robot physical and sensing parameters* and the *robot population* that will provably achieve boundary coverage statistics that may be of interest in multi-robot applications. As stated previously, we assume that the robots have no global position information, no inter-robot communication, and no prior information about the boundary location or geometry. First, we derive the probability that a robot configuration around a boundary is *saturated*, meaning that each adjacent pair of robots lies within a certain distance. The quantity that this distance signifies depends on the application. For instance, when saturation corresponds to full sensor coverage of the boundary, the distance represents the

[1]Ganesh P. Kumar is with the School of Computing, Informatics, and Decision Systems Engineering, Arizona State University, Tempe, AZ 85287, USA gpkumar@asu.edu

[2]Spring Berman is with the School for Engineering of Matter, Transport and Energy, Arizona State University, Tempe, AZ 85287, USA spring.berman@asu.edu

978-1-4799-3684-7/14/$31.00 ©2014 IEEE

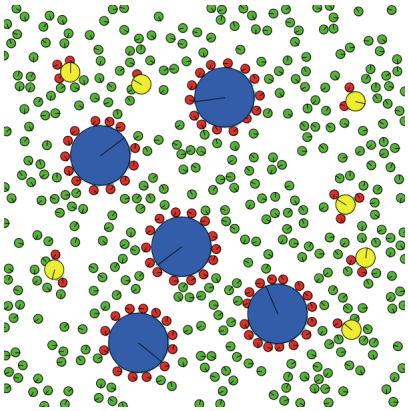

Fig. 1. Snapshot of a simulation in which a swarm of randomly-moving robots (green circles) with only local information must allocate themselves in groups of target sizes (red circles) around the perimeters of two types of circular regions (yellow and blue). We have developed an approach to designing stochastic robot control policies that produce the target allocations with probabilistic guarantees on performance [19].

diameter of a robot's sensing range. Using order statistics, we also derive the probability distributions of robot positions along the boundary and distances between adjacent robots.

In this paper, we consider scenarios in which robots are positioned at uniformly random positions along the boundary. The analytical results that we develop for this case would apply to scenarios in which robots are confined to the boundary at unknown locations or arrive simultaneously at the boundary at random positions. We study this case as a foundation for future work on analyzing the more general case in which robots claim positions along the boundary one at a time, as in the scenario in Figure 1.

II. Problem Statement

Let $\mathscr{I} = [0,1]$ be the unit interval. We are given a simple open or closed curve $\gamma : \mathscr{I} \to \mathbb{R}^2$ that has unit length. In addition, if closed, γ is parameterized such that $\gamma(0) = \gamma(1)$. A sequence of n identical circular robots, each of radius $\delta \geq 0$, is placed at random positions along γ, with no overlapping robot pairs. By the position of a robot, we mean that of its center. The robot positions $\gamma(t'_1)$ through $\gamma(t'_n)$, not necessarily arranged in order, are provided to us; we are further given that, if γ is closed, we have $\gamma(0) = \gamma(t'_1)$. For our convenience, we call robots of zero radius *point robots*, and those with $\delta > 0$ *finite-sized* robots.

Define the distance between two robots to be the closest distance between their circles. This implies that the distance between two robots located at positions $\gamma(t'_1)$ and $\gamma(t'_2)$ is the absolute value of $||\gamma(t'_2) - \gamma(t'_1)|| - 2\delta$. Given a positive distance $d \in \mathscr{I}$, we define the notion of *saturation* separately for open and closed curves. The closed curve γ is defined to be saturated iff every pair of adjacent robots on it is separated by a distance of at most d. The open curve γ is defined to be saturated iff, in addition to having adjacent robots separated by at most d, the centers of the first and and last robots on γ leave a distance of at most d from the endpoint of γ closest to them.

For finite-sized robots of radius δ, we generally choose a value of d that ensures that no robot will fit in between two adjacent robots whose distance is at most d. Evidently, the choice $d = 2\delta$ ensures this, and will be used hereafter. No such d naturally suggests itself for point robots, for whom d can be selected arbitrarily. With this in mind, we formulate our problem.

Problem Statement Given a configuration in which each of n robots uniformly randomly attach to γ, compute:

1) the probability p_{sat} that they saturate the curve,
2) the probability density functions (pdf's) of each robot on the curve, and
3) the pdf of the inter-robot distance between adjacent robots.

Note that this statement deals with four cases, for the robots can be either point or finite-sized, and the curve can be either closed or open. Our next step will be to save labor by cutting down these four cases to two.

III. Reduction from Open to Closed Curve

In this section, we reduce any problem for a robot configuration on an open curve to an equivalent one on a closed curve, thereby simplifying our computations. Suppose first that γ is closed. Cut γ open at $\gamma(0) = \gamma(1)$, and unwrap it on the positive real axis, placing $\gamma(0)$ at zero. Since γ has unit length, it unwraps completely onto the unit interval $\mathscr{I}$. Note that unwrapping γ leaves distances between robots unchanged. The robot positions $\gamma(t'_i)$ now fall on positions t'_i on $\mathscr{I}$. Observe that t'_1 is identified with *both* endpoints of $\mathscr{I}$, as γ was a closed curve. We will use this important property repeatedly in the coming discussion.

Now start at t'_1 and move rightwards along $\mathscr{I}$, labeling robot positions in order until the right endpoint of $\mathscr{I}$ is reached, taking us back to t'_1. This results in the sequence $(t_1 = t'_1, t_2, \ldots, t_n)$, which is a permutation of the unordered points t'_i. Since $t_1 = t'_1$ is identified with both ends of $\mathscr{I}$, it is considered to fall to the left of t_2, as well as to the right of t_n, at the same time. Thus, the distance between t_1 and t_2 uses $t_1 = 0$, and equals t_2; on the other hand, the distance between t_n and t_1 makes use of $t_1 = 1$, and evaluates to $1 - t_n$. To make results simple, we define $t_{n+1} = t_1$, pretending that the index wraps around. Also, use the value $t_{n+1} = 1$ when computing the distance $t_{n+1} - t_n$. Saturation requires each inter-robot distance of the form $t_{i+1} - t_i$ to be bounded above by d.

Next, suppose that γ is an open curve, to which n robots attach precisely as before. Unwrap the curve as before onto $\mathscr{I}$. Because γ is open, we have $t'_1 \neq 0$ in general. Consequently, labeling robot positions in order leads to $t_1 \neq 0$ in general. Like in the case of closed curves, saturation implies that $t_{i+1} - t_i \leq d$, for $1 \leq i \leq n-1$. However, since γ is open, saturation forces two additional constraints: $t_1 \leq d$ and $1 - t_n \leq d$.

Introduce an *artificial* point robot t_0, and identify it with both ends of $\mathscr{I}$. This robot behaves exactly like t_1 in the case of closed γ. Define $t_{n+1} = t_0$, analogous to closed curves, except that the index wraps back to 0 instead of 1. As before, always take $t_{n+1} = 1$ for computing $t_{n+1} - t_n$. Now

saturation needs $t_1 - t_0 \leq d$, and $t_{n+1} - t_n = 1 - t_n \leq d$, which are equivalent to the two extra constraints. This scenario is identical to having $n+1$ robots on a closed curve. Also, note that the position of t_i on the open curve matches that of t_{i+1} on the closed curve.

An additional observation helps us with the reduction for *finite-sized* robots. Suppose that the closed curve γ having n finite-sized robots is unwrapped on $\mathscr{I}$ as before. The first robot centered at $t_1' = t_1 = 0$ splits in half when γ unwrapped. It spans the endpoints of $\mathscr{I}$ to occupy the disconnected interval $F_1 = [0,\delta] \cup [1-\delta, 1]$, splitting into half-circles. Every other robot is centered at some $t_i \in \mathscr{I}$, and physically occupies the interval $F_i = [t_i - \delta, t_i + \delta]$ now. Define $t_{n+1} = t_1$ as before, pretending that the index wraps around. Note that the n robots take up a length of $2\delta n$ altogether on $\mathscr{I}$. For saturation, we require that no robot can fit in the space between two consecutive ones. This leads n constraints of the form $t_{i+1} - t_i < 2\delta$.

When γ is open, however, $t_1 \neq 0$ in general, leading to two extra constraints , $t_1 < 2\delta$ and $1 - t_n < 2\delta$. As before, we introduce the artificial robot t_0; however, it must be placed in a way that resembles that of t_1 for closed curves, yet does not take away any space from $\mathscr{I}$ for other robots to occupy. To meet both these requirements, we place t_0 *outside* $\mathscr{I}$, splitting it into half-circles so that $F_0 = [-\delta, 0] \cup [1, 1+\delta]$. Also, we have $t_{n+1} = 1$, coinciding with the right endpoint of $\mathscr{I}$. For saturation, t_1 can be at most δ away from t_0, and likewise t_n can be at most δ away from t_{n+1}, taking care of the two extra constraints automatically. This is equivalent to having $n+1$ robots on a closed curve of length $1+2\delta$.

In short, for point robots, a problem with parameters (n,d) on the open curve is equivalent to one with parameters $(n+1,d)$ on the closed curve. For finite-sized robots, a problem with parameters (n,δ) on the open curve of unit length is equivalent to one with parameters $(n+1,\delta)$ on a closed curve of length $1+2\delta$. Due to these reductions, the future sections will compute results mainly for closed curves, commenting on the open curve case only when needed.

IV. A Brute Force Approach to Computing p_{sat}

We now turn back to n point robots on a closed curve. We first characterize p_{sat} as the ratio of the measure of $\mathscr{E}$, the space of saturated robot configurations, to the measure of Ω, the sample space of all possible robot configurations. Since $t_1 = 0$, the sample space Ω consists of all points $(t_2, t_3, \ldots, t_n)$ with coordinates obeying $0 \leq t_i \leq t_{i+1} \leq 1$. This space Ω forms a simplex in $\mathbb{R}^{n-1}$ with vertices $v_1 = (0,0,\ldots,0,0), v_2 = (0,0,\ldots,0,1), v_3 = (0,0,\ldots,0,1,1), \ldots, v_n = (1,1,\ldots,1,1)$. We call Ω the *event simplex*. The measure of Ω is its $(n-1)$-dimensional volume,

$$|\Omega| = \int_0^1 \int_{t_2}^1 \ldots \int_{t_{n-1}}^1 dt_n \ldots dt_3 dt_2 = \frac{1}{(n-1)!} \tag{1}$$

We now characterize the space $\mathscr{E}$ of *saturated* robot configurations. To do this, we need to identify the set of robot position ranges, or *saturating intervals* I_i, $i = 2, ..., n$, that guarantee a saturated robot configuration. We derive the I_i from the intersection of the *left saturating interval* L_i and *right saturating interval* R_i for each robot position t_i. These two intervals denote the range of positions that result in the saturating conditions $(t_i - t_{i-1}) \in [0,d]$ and $(t_{i+1} - t_i) \in [0,d]$, respectively.

To ensure the condition $(t_i - t_{i-1}) \in [0,d]$, we define the left saturating interval for each robot position t_i as

$$L_i = [t_{i-1}, \min(t_{i-1} + d, 1)], \qquad i = 2, 3, \ldots, n \tag{2}$$

To ensure the condition $(t_1 - t_n) = (1 - t_n) \in [0,d]$, we define the right saturating interval for position t_n as

$$R_n = [\max(0, 1-d), 1] \tag{3}$$

We obtain the right saturating intervals R_i for the remaining positions t_i using the following approach. We will refer to a sequence of robot positions as *d-separated* if the distance between any two consecutive robot positions is precisely d. Consider a particular $t_2 \in L_2$, and define a sequence of d-separated positions $t_3, t_4, \ldots, t_n$. If the resulting $t_n \in R_n$, the choice of t_2 is sufficient to ensure saturation. The leftmost possible positions t_i that will still result in saturation are $t_n = 1 - d, t_{n-1} = 1 - 2d, \ldots, t_2 = 1 - (n-1)d$. Hence, to ensure saturation, we define $R_2 = [\min(1 - d(n-1), 0), 1]$. Extending this reasoning to the remaining robot positions, the following R_i ensure the condition $(t_{i+1} - t_i) \in [0,d]$:

$$R_i = [\min(1 - (n-i+1)d, 0), 1], \qquad i = 2, 3, \ldots, n-1 \tag{4}$$

Finally, from the intervals in Equation (2), Equation (3), and Equation (4), we obtain the following intervals for the robot positions that lead to saturated configurations:

$$I_i = L_i \cap R_i = [\max(t_{i-1}, 1 - (n-i+1)d), \min(t_{i-1} + d, 1)], \quad i = 2, 3, \ldots, n \tag{5}$$

A point in $\mathscr{E}$ has $t_i \in I_i$ for $i \in \{2, 3, \ldots, n\}$. We can compute the measure of $\mathscr{E}$ as

$$|\mathscr{E}| = \int_{t_2 \in I_2} \int_{t_3 \in I_3} \ldots \int_{t_n \in I_n} dt_n \ldots dt_2 \tag{6}$$

Note that if any of the intervals I_i is empty, $\mathscr{E}$ becomes the empty set and the probability of saturation is zero.

This integral can be evaluated on a case-by-case basis, but a naive expansion of the min and max functions in the limits of each I_i could result in an exponential number of subintegrals, which is computationally expensive. Thus, the probability of saturation $p_{sat} = |\mathscr{E}|/|\Omega|$ needs to be determined by other means, for which we explore the geometric approach described in the next section.

V. Geometric Interpretation of p_{sat}

We use an approach to computing p_{sat} that can be described geometrically and is based on the characterization of the inter-robot distances, which we call the *slacks*. We will initially consider configurations of *point robots*. Given a sequence of robot positions t_i, $i = 1, 2, \ldots, n$, define the i^{th} slack to be the distance between t_i and t_{i+1}:

$$s_i = t_{i+1} - t_i, \qquad i = 1, 2, \ldots, n \tag{7}$$

$$\tag{8}$$

Recall from section III that since $t_{n+1} = 1$, we have $s_n = 1 - t_n$. Define the *slack set* $S_n \subset \mathbb{R}^n$ to be the set of all possible *slack points* $\mathbf{s} = (s_1, s_2, \ldots, s_n)$, each of whose components is a valid slack. To characterize this set, we note that valid slacks are always nonnegative and that the sum of the slacks, called the *total slack* s, is always equal to the curve length l. Thus, the slack set is defined as

$$S_n = \{\mathbf{s} \in \mathbb{R}^n \mid s_i \geq 0,\ i = 1, 2, \ldots, n,\ \sum_{i=1}^{n} s_i = s\} \quad (9)$$

The slack set S_n forms an $(n-1)$-dimensional simplex that we call the *slack simplex*. The n vertices of S_n are located at $(s, 0, 0, \ldots, 0), (0, s, 0, \ldots, 0), \ldots, (0, 0, 0, \ldots, s)$. Hence, S_n is a regular simplex with side length $s\sqrt{2}$. The volume of an n-dimensional regular simplex of side a is

$$V_n(a) = \left(\frac{a}{\sqrt{2}}\right)^n \frac{\sqrt{n+1}}{n!} \quad (10)$$

This gives the following volume for S_n:

$$|S_n| = V_{n-1}(s\sqrt{2}) = \frac{s^{n-1}\sqrt{n}}{(n-1)!} \quad (11)$$

Now we describe the set of points $\mathbf{s} \in \mathbb{R}^n$ that corresponds to configurations that are saturated, but that do not necessarily conserve the total slack (and thus form a valid robot configuration). For such configurations, $s_i \in [0, d]$ for all i. Thus, the set of all points leading to saturation forms an n-dimensional hypercube H_n:

$$H_n = \{\mathbf{s} \in \mathbb{R}^n \mid 0 \leq s_i \leq d,\ i = 1, 2, \ldots, n\} \quad (12)$$

The set of valid robot configurations that are saturated is therefore the $(n-1)$-dimensional set $E_n \equiv S_n \cap H_n$. The probability of saturation p_{sat} is the volume of this set divided by the volume of the slack simplex, the set of all valid robot configurations. Determining the volume of E_n is not straightforward, but it can be computed using the following approach. Suppose that $A_k \subseteq \{1, 2, \ldots, n\}$ is a k-element subset of the slack indices. Define for any A_k the set $E'_n(A_k)$ consisting of all slack points whose components s_i, $i \in A_k$, are at least d:

$$E'_n(A_k) = \{\mathbf{s} \in S_n \mid s_i \geq d\ \forall i \in A_k\} \quad (13)$$

Note that there is no constraint on the remaining slack coordinates, which may exceed or fall below d as long as $\mathbf{s} \in S_n$. For each slack s_i, $i \in A_k$, define a *reduced slack* $s'_i = s_i - d$. We can equivalently define $E'_n(A_k)$ in terms of the reduced slacks as:

$$E'_n(A_k) = \{\mathbf{s} \in S_n \mid \sum_{i \in A_k} s'_i + \sum_{i \notin A_k} s_i = s - kd\} \quad (14)$$

This definition makes it evident that $E'_n(A_k)$ is a regular simplex that conserves the total reduced slack $s - kd$. By Equation (10), its $(n-1)$-dimensional volume is given by

$$|E'_n(A_k)| = V_{n-1}((s-kd)\sqrt{2}) = \frac{(s-kd)^{n-1}\sqrt{n}}{(n-1)!} \quad (15)$$

Equation (15) makes sense only if $(s - kd) \geq 0$; equivalently, we need $1 \leq k \leq K$ where $K = \lfloor s/d \rfloor$. If $k > K$, then $|E'_n(A_k)| = 0$, as there is no subset of S_n in which $s_i > d$, $i \in A_k$. We will next use Equation (15) to compute the volume of $E'_n = S_n \backslash E_n$. This set is defined as

$$E'_n = \{\mathbf{s} \in S_n \mid \exists s_i \geq d,\ i \in \{1, 2, \ldots, n\}\} = \bigcup_{A_k} E'_n(A_k) \quad (16)$$

Note that the union runs over all possible choices of A_k. To compute the volume of the union, we use the *Inclusion-Exclusion Principle* [20] which states that

$$|\bigcup_{A_k} E'_n(A_k)| = \sum_{k=1}^{n} (-1)^{k-1} \sum_{k=1}^{n} |E'_n(A_k)| \quad (17)$$

To evaluate the second sum on the righthand side of Equation (17), note that there are precisely $\binom{n}{k}$ subsets of $\{1, 2, \ldots, n\}$ of cardinality k, and the volume of each corresponding $E'_n(A_k)$ is given by Equation (15). Also, we need to take this sum only on the range $1 \leq k \leq K$, for otherwise $|E'_n(A_k)| = 0$. From these observations, we obtain

$$|E'_n| = |\bigcup_{A_k} E'_n(A_k)| = \sum_{k=1}^{K} (-1)^{k-1} \binom{n}{k} \frac{(s-kd)^{n-1}\sqrt{n}}{(n-1)!} \quad (18)$$

Since $E_n = S_n \backslash E'_n$, $|E_n| = |S_n| - |E'_n|$. Using Equation (11) and Equation (18), we obtain the probability of saturation:

$$p_{sat} = \frac{|E_n|}{|S_n|} = 1 - \sum_{k=1}^{K} (-1)^{k-1} \binom{n}{k} \left(1 - \frac{kd}{s}\right)^{n-1} \quad (19)$$

Finally, from section III, this result trivially extends to open curves by mapping $n \mapsto n+1$.

A. Evaluating the Intractable Integral in Equation (6)

An immediate consequence of Equation (19) is that we can now evaluate the integral in Equation (6) as $|\mathscr{E}| = p_{sat}|\Omega| = p_{sat}/(n-1)!$ Let Σ denote the sum on the right side of Equation (19). Given n, d, and $s = 1$, this sum Σ Equation (19) takes K steps in all to evaluate in a loop. For efficiency, the k-th step computes $\binom{n}{k}$ recursively from $\binom{n}{k-1}$ in $O(1)$ time and the power term $(1 - kd/s)^{n-1}$ by binary exponentiation in $O(\log n)$ time. Note that both $\binom{n}{k}$ and the power term have a size that is bounded above by a polynomial function of the number of input bits. As such, p_{sat} can be computed in polynomial time, with $O(K \log n)$ multiplications in all.

B. Extension to Finite-Sized Robots

We avoided addressing finite-sized robots in section IV, since this case is even more complicated than that of point robots. However, the geometric approach has an easy extension to finite-sized robots. Following section II, define the slack s_i by

$$s_i = t_{i+1} - t_i - 2\delta,\ i = 1, 2, \ldots, n \quad (20)$$

where as usual $t_{n+1} = 1$. Given t_i and s_i, the next robot is located at $t_{i+1} = t_i + s_i + 2\delta$ and occupies the interval $F_{i+1} = [t_i + s_i + \delta, t_i + s_i + 3\delta]$.

No matter how the robots are positioned, the total length of the curve not occupied by robots is $1-2\delta n$. In addition, in saturated robot configurations, all slacks s_i are too small to fit another robot between the robots at t_i and t_{i+1}; that is, $s_i \in [0, 2\delta]$. Hence, we have the following values for the total slack s and the saturating distance d:

$$s = 1-2\delta n \quad (21)$$
$$d = 2\delta \quad (22)$$

Using the same reasoning as in the point robot case, the set of possible slack points for finite-sized robot configurations consists of the slack simplex Equation (9) with s defined in Equation (21), and the set of all points corresponding to saturated configurations forms the hypercube Equation (12) with d defined in Equation (22). Repeating the analysis developed for point robots, we find that the formula for p_{sat} is given by Equation (19) with the newly defined values of s and d.

Finally, we comment briefly about the analogous results for open curves. The reduction in section III from open to closed curves, causes γ to lengthen by 2δ, and the new slack becomes

$$s = 1-2\delta(n-1) \quad (23)$$

Also, the number of robots gets incremented during the reduction, giving us

$$p_{sat} = 1-\sum_{k=1}^{K}(-1)^{k-1}\binom{n+1}{k}\left(1-\frac{kd}{s}\right)^n \quad (24)$$

where $K := \lfloor \frac{s}{d} \rfloor$ uses the slack of Equation (23).

VI. Statistics of Robot Positions and Slacks

The problem of computing the statistics of the robot positions t_i and the slacks s_i can be approached using results from *order statistics* [21]. The unordered points t'_i, which were picked uniformly randomly on the unit interval $\mathscr{I}$, are called the *parent* variables; the i^{th} ordered point t_i is called the i^{th} *order statistic* of the parent. An approach based on order statistics not only confirms Equation (19) [21, pp.133-135] but also yields the pdf's of t_i and s_i. To simplify notation, we define the *indicator function* $\mathbf{1}_X : X \to \{0,1\}$ of an arbitrary set X to be $\mathbf{1}_X(x) := 1$ iff $x \in X$, and $\mathbf{1}_X(x) := 0$ otherwise. We also use f to denote a pdf, which may be either joint or marginal.

A. Statistics of Point Robots

We begin with the case of n point robots. From the problem statement, we have that the joint pdf of the parents $f(t'_1, t'_2, \ldots, t'_n)$ is uniform over its domain, which is the event simplex Ω. Since from Equation (1), $|\Omega| = 1/(n-1)!$, we need

$$f(t'_1, t'_2, \ldots, t'_n) = (n-1)!\mathbf{1}_\Omega \quad (25)$$

to ensure that $f(t'_1, t'_2, \ldots, t'_n)$ has unit measure over Ω and thus is a pdf.

Since the order statistics t_i are just a permutation of their parents, their joint pdf $f(t_1, t_2, \ldots, t_n)$ is identical to that of their parents. Note that t_1 is fixed and thus has a degenerate marginal pdf, and we omit it from further consideration. We can obtain the pdf of other order statistic $t_i : i = 2, 3, \ldots, n$, by repeatedly marginalizing over the remaining $n-2$ statistics. We do so in two steps. In the first step, notice that the order statitics $t_j : j = i+1, i+2, \ldots, n$ to the right of t_i each need to be integrated over the interval $R_j = [t_{j-1}, 1]$. This leads us to a marginal density of the form $f(t_2, \ldots, t_i)$, consisting only of t_i and the statistics to its left. Next, we marginalize away the statistics $t_k : k = 2, \ldots, i-1$ to the left of the desired one by integrating each of them over the intervals $L_k = [0, t_i]$. This gives the result

$$f(t_i) = \int_{L_k}\int_{R_j} f\,dt_n \ldots dt_{i+1}dt_{i-1}\ldots dt_2 = \binom{n}{i}(1-t_i)^{n-i}t_i^{i-1} \quad (26)$$

where we wrote

$$\int_{L_k} \text{ for } \int_{t_1\in L_1}\int_{t_2\in L_2}\cdots\int_{t_{i-1}\in L_{i-1}},$$
$$\int_{R_j} \text{ for } \int_{t_{i+1}\in R_{i+1}}\int_{t_{i+2}\in R_{i+2}}\cdots\int_{t_n\in R_n},$$

and f for the joint density of the order statistics.

Define the *Beta* density [22, pp.42-43] $\text{Beta}(t|a,b)$ by

$$\text{Beta}(t|a,b) := \frac{1}{B(a,b)}t^{a-1}(1-t)^{b-1}\mathbf{1}_{\mathscr{I}} \quad (27)$$

This density has mean and variance given by

$$E[\text{Beta}(t|a,b)] = \frac{a}{a+b}$$
$$Var[\text{Beta}(t|a,b)] = \frac{ab}{(a+b+1)(a+b)^2}$$

Then it is easy to see that each order statistic is a Beta variate of the form

$$f(t_i) = \text{Beta}(t_i|i, n-i+1) \quad (28)$$

with mean and variance given by

$$E[t_i] = \frac{i-1}{n} \quad (29)$$
$$Var[t_i] = \frac{(i-1)(n-i+1)}{n^2(n+1)} \quad (30)$$

Intuitively, Equation (28) indicates that t_i is the $(i-1)^{\text{st}}$ variable from among the $n-1$ picked on $\mathscr{I}$. The $n-1$ order statistics t_2 through t_n divide $\mathscr{I}$ into n subintervals. On average, these subintervals have equal length, placing the expected location of t_i at $\frac{i-1}{n}$.

We next compute the pdf's of the slacks. Note that any particular slack, say the last slack s_n, can be determined as a function of the remaining ones, as $s_n = 1-\sum_{i=1}^{n-1} s_i$. To define the joint pdf of the slacks, keep this slack apart, and define the domain

$$D := \{(s_1, s_2, \ldots, s_{n-1})\} : 0 \le s_i \le 1, 0 \le \sum_{i=1}^{n-1} s_i \le 1 \quad (31)$$

This domain is the interior of an $(n-1)$ dimensional simplex embedded in $\mathbb{R}^{n-1}$ and is easily seen to have the $(n-1)$-dimensional volume $|D| = \frac{1}{(n-1)!}$ by a nested integral identical to Equation (1), leading to the joint pdf

$$f(s_1, s_2, \ldots, s_{n-1}) = (n-1)!\mathbf{1}_D \tag{32}$$

Unlike the order statistics which need $t_i \leq t_{i+1}$, the slacks have no such restriction. Since any reordering of slacks makes no difference to Equation (32), every slack has the same marginal pdf by symmetry. This includes the slack s_n that was omitted from the joint pdf, for we could have set up Equation (25) by setting apart another slack, say s_{n-1} instead. Thus we need to determine only one marginal pdf, say $f(s_1)$. To do so, we follow a marginalization process similar to that for the order statistics. Note that every slack $s_j : j = 2, \ldots, n-1$ to the right of s_1 lies on the interval $R_j = [0, 1 - \sum_{i=1}^{j-1} s_j]$. Integrating the joint slack pdf in Equation (32) over these intervals leads us to

$$f(s_i) = \text{Beta}(s_i|1, n-1), i = 1, 2, \ldots, n \tag{33}$$

We add a note of caution here that will become relevant to the case of finite-sized robots. Observe that since $t_i = \sum_{j=1}^{i-1} s_j$, it may be tempting to compute the marginal density $f(t_i)$ by performing $i-1$ nested convolutions of the slack pdf's. However, it can be seen while computing the marginal pdf's that slacks are mutually dependent, so that for example $f(s_1, s_2) \neq f(s_1)f(s_2)$. Deriving $f(s_i)$ by repeated integration sidesteps this issue of dependency.

Finally, all results from Equation (25) through Equation (33) extend trivially to open curves as follows. Since the reduction process from open to closed curves increments the number of robots, the joint pdf for n robots on an open curve is

$$f(t_1, t_2, \ldots, t_n) = n!\mathbf{1}_\Omega \tag{34}$$

where Ω is now an n-dimensional simplex embedded in $\mathbb{R}^n$. The statistic t_i for a closed curve resembles that of t_{i+1} for closed curves, giving us

$$f(t_i) = \text{Beta}(t_i|i, n-i+1), \; i = 1, 2, \ldots, n \tag{35}$$

$$f(s_i) = \text{Beta}(t_i|1, n), \; i = 1, 2, 3, \ldots, n+1 \tag{36}$$

B. Extension to Finite-Sized Robots

In the case of finite-sized robots, the slacks s_i are the order statistics of points uniformly randomly chosen on the interval $[0, s = 1 - 2\delta n]$. Had s been unity, the pdf of each s_i would have been given by the Beta pdf in Equation (33). If we divide each s_i by s, the scaled random variables s_i/s will be distributed over $\mathscr{I}$ according to this Beta pdf. From this, we derive the following expressions for the pdf of s_i:

$$f(s_i) = s \cdot \text{Beta}(t|1, n-1) \tag{37}$$

However, determining the pdf of t_i does not readily admit an analytic form. Having set $t_1 = 0$, from Equation (20) we know that

$$t_2 - 2\delta = s_1 \tag{38}$$

Consequently, $t_2 - 2\delta$ will have the same pdf as s_1, or

$$f(t_2) = s \cdot \text{Beta}(t|1, n-1) + 2\delta \tag{39}$$

The case of t_3 is different. From Equation (20),

$$t_3 - 4\delta = s_1 + s_2 \tag{40}$$

Determining $f(t_3)$ by convoution fails due to the fact that slacks are dependent, as the note of caution makes clear in section VI-A. Unlike with point robots, we do not have a general expression for the joint pdf of finite-sized ones. Thus, the marginalization procedure of section VI-A fails, and we have no analytic expressions for the pdf of t_3 through t_n.

VII. Simulations

We implemented Monte Carlo simulations in which various numbers n of either point robots or finite-sized robots are stochastically allocated to the boundary of a unit circle. In the point robot simulations, n points were chosen uniformly randomly from $\mathscr{I}$ and sorted in order. The slacks were computed, and those robot configurations that met the saturation criterion were counted as favorable events. The finite-sized robots implemented the following algorithm:

Algorithm SLACK-ATTACH(n, δ)

1) Set $t_1 \leftarrow 0$.
2) Pick an array $arr[1..n-1]$ of uniformly randomly distributed points on the interval $[0, s]$.
3) Sort arr in increasing order.
4) Compute the individual slacks as $s_1 \leftarrow arr[1]$, $s_i \leftarrow arr[i+1] - arr[i]$ for $2 \leq i \leq n-1$, and $s_n \leftarrow s - \sum_{1 \leq i \leq n-1} s_i$.
5) Compute $t_{i+1} = t_i + s_i + 2\delta$ for $1 \leq i \leq n-1$.

Robot configurations that satisfied $s_i = d \leq 2\delta$ were counted as favorable events.

Figure 2 compares three-dimensional plots of theoretical and Monte Carlo-averaged (over 20000 trials) p_{sat} varying with n and d for point and finite-sized robots. For both robot types, the close match between the theoretical and Monte Carlo-averaged plots validate our formula for p_{sat}. Table I and Table II show a quantitative comparison of p_{sat} computed from Equation (19) and p_{sat} averaged over 20000 Monte Carlo trials for different combinations of n and d. Table III and Table IV display the corresponding results for finite-sized robots. For both robot types, the theoretical predictions of p_{sat} closely match the Monte Carlo simulation averages.

We also plotted the frequency of 5000 samples of a particular robot position and a particular slack from Monte Carlo trials with $n = 5$ point robots. As Figure 3 shows, both frequency plots can be fit to the Beta densities predicted by Equation (28) and Equation (37).

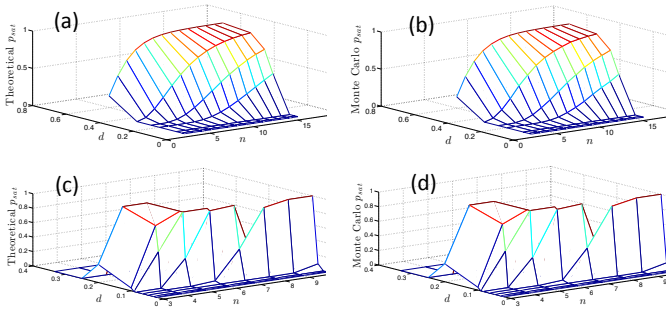

Fig. 2. Plots of theoretical (left column) and Monte Carlo-generated (right column) $p_{sat}(n,d)$ values for point (upper row) and finite-sized (lower row) robots.

TABLE I

THEORETICAL p_{sat} VS. p_{sat} MONTE CARLO-AVERAGED WITH $n = 16$ POINT ROBOTS

d	Theoretical p_{sat}	Monte Carlo p_{sat}
0.05	0.0000	0.0000
0.10	0.0001	0.0001
0.20	0.4929	0.4925
0.25	0.7898	0.7913
0.33	0.9635	0.9651
0.5	0.9995	0.9997

TABLE II

THEORETICAL p_{sat} VS. MONTE-CARLO AVERAGED p_{sat} TRIALS WITH POINT ROBOTS, WITH $d = 0.5$

n	Theoretical p_{sat}	Monte Carlo p_{sat}
3	0.2500	0.2467
4	0.5000	0.5029
5	0.6875	0.6885
6	0.8125	0.8124
7	0.8906	0.8899
8	0.9375	0.9383

TABLE III

THEORETICAL p_{sat} VS. MONTE CARLO-AVERAGED p_{sat} WITH $n = 4$ FINITE-SIZED ROBOTS

δ	Theoretical p_{sat}	Monte Carlo p_{sat}
0.05	0.0000	0.0000
0.06	0.0029	0.0025
0.08	0.5000	0.5060
0.09	0.8519	0.8532
0.1	1.0000	1.0000

TABLE IV

THEORETICAL p_{sat} VS. MONTE CARLO-AVERAGED p_{sat} TRIALS WITH FINITE-SIZED ROBOTS, WITH $\delta = d/2 = 0.05$

n	Theoretical p_{sat}	Monte Carlo p_{sat}
5	0.000	0.000
6	0.0254	0.0259
7	0.4142	0.4221
8	0.9375	0.9401

VIII. CONCLUSIONS AND FUTURE WORK

We have demonstrated approaches to the statistical analysis of quantities that are associated with stochastic coverage of a simple boundary by a set of uniformly randomly

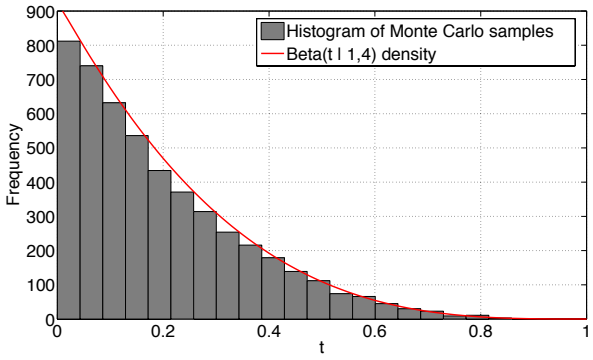

(a) Frequency plot of t_2

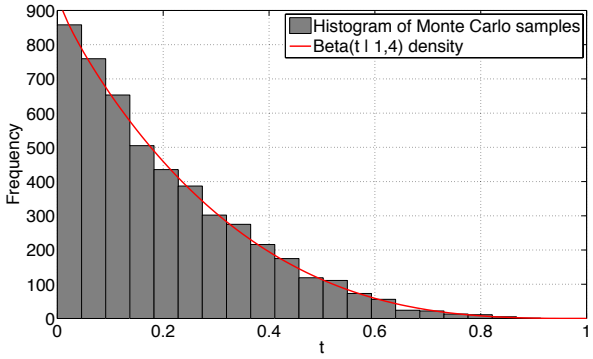

(b) Frequency plot of s_2

Fig. 3. Frequency plots of 5000 samples of t_2 and $s_2 = t_3 - t_2$ from Monte Carlo trials for point robots Both plots are fit to a Beta$(t|1,4)$ density function.

distributed robots. We developed a geometric interpretation of the probability that a given robot configuration is saturated and derived this probability using the Inclusion-Exclusion Principle. We also used results from order statistics to determine the probability distributions of the robot positions along the boundary and the distances between adjacent robots. We validated our derived formulas for these probability distributions and the saturation probability using Monte Carlo simulations of a large number of scenarios. The work presented here can be extended in several directions:

a) Stochastic coverage by asynchronously attaching robots: Many experimental scenarios will involve asynchronous attachment of robots to a boundary. In these cases, each attaching robot searches for an available attachment location on the boundary and picks one at random. One possible algorithm for simulating this process with finite-sized robots is as follows:

Algorithm ASYNC-ATTACH(n, δ)

1) Set $t_i' \leftarrow 0$
2) For each $i : 2 \leq i \leq n$ do
   a) Find the list of intervals in which the center t_i' of the next robot can be placed.
   b) Choose one such interval at random and one point p at random from this interval.

c) Set $t_i' \leftarrow p$.

3) Sort t_i' in increasing order to get t_i.

The parent variables t_i' assigned by ASYNC-ATTACH are not i.i.d, since each t_i' is a function of $t_1', t_2', \ldots, t_{i-1}'$. This makes the determination of their order statistics a much more challenging task [21, Ch.5] for which a complete analytical solution may be impossible. Hence, an important future step would be to extract useful qualitative information about the distributions generated by ASYNC-ATTACH and other asynchronous attachment algorithms. Also pertinent would be to devise asynchronous attachment algorithms that lend themselves to tractable analysis.

b) Probability distributions induced by saturation: As an extension of the material in Section VI, we plan to derive the pdf's of t_i and s_i given that the robot configuration is saturated.

c) Comparison with deterministic algorithms: Multi-robot planar boundary coverage is an NP-Hard problem [23]. Deterministic algorithms for this problem generally employ heuristics to reduce running time. Our approach is essentially a randomized algorithm to address the same intractability. Deterministic algorithms provide more guarantees on run-time and correctness than randomized algorithms, while the latter may be simpler to implement [24]. Our future work will investigate scenarios that favor one approach over the other; for example, we would wish to determine the better coverage approach when collisions with obstacles or between robots need to be avoided.

d) Applications to multi-robot transport problems: We are currently investigating the problem of developing strategies for multi-robot collective transport that are robust to payload type, environment layout, and transport team size, much like group retrieval strategies employed by certain species of ants [25]. We will consider scenarios in which robots stochastically allocate themselves around a payload and then proceed to transport the payload as a team. We will apply our statistical analysis results to characterize dynamical properties of the robot-load system during transport given an initial stochastic allocation. For instance, we can investigate the probability that robots arranged in a random configuration around a certain payload will be able to successfully lift it off the ground.

ACKNOWLEDGMENTS

We are grateful to Dr. Theodore P. Pavlic and Sean Wilson for useful discussions on the material presented in this paper.

REFERENCES

[1] V. Kumar and N. Michael, "Opportunities and challenges with autonomous micro aerial vehicles," *Int'l. Journal of Robotics Research*, vol. 31, no. 11, pp. 1279–1291, 2012.

[2] K. Y. Ma, P. Chirarattananon, S. B. Fuller, and R. J. Wood, "Controlled flight of a biologically inspired, insect-scale robot," *Science*, vol. 340, no. 6132, pp. 603–607, 2013.

[3] E. Diller and M. Sitti, "Micro-scale mobile robotics," *Foundations and Trends in Robotics*, vol. 2, pp. 143–259, 2013.

[4] S. Tong, E. Fine, Y. Lin, T. J. Cradick, and G. Bao, "Nanomedicine: Tiny particles and machines give huge gains," *Annals of Biomedical Engineering*, pp. 1–17, 2013.

[5] C. Mavroidis and A. Ferreira, "Nanorobotics: Past, present, and future," in *Nanorobotics*, C. Mavroidis and A. Ferreira, Eds. Springer New York, 2013, pp. 3–27.

[6] S. Hauert, S. Berman, R. Nagpal, and S. N. Bhatia, "A computational framework for identifying design guidelines to increase the penetration of targeted nanoparticles into tumors," *Nano Today*, vol. 8, no. 6, pp. 566–576, 2013.

[7] S. Wang and E. E. Dormidontova, "Selectivity of ligand-receptor interactions between nanoparticle and cell surfaces," *Phys. Rev. Lett.*, vol. 109, p. 238102, Dec 2012.

[8] L. Matthey, S. Berman, and V. Kumar, "Stochastic strategies for a swarm robotic assembly system," in *Proceedings of the 2009 IEEE International Conference on Robotics and Automation*, Kobe, Japan, May 12–17, 2009, pp. 1953–1958.

[9] W. C. Evans, G. Mermoud, and A. Martinoli, "Comparing and modeling distributed control strategies for miniature self-assembling robots," in *Int'l. Conf. Robotics and Automation (ICRA)*, 2010, pp. 1438–1445.

[10] E. Klavins, S. Burden, and N. Napp, "Optimal rules for programmed stochastic self-assembly," in *Proceedings of Robotics: Science and Systems*, Philadelphia, PA, USA, August 2006.

[11] N. Napp, S. Burden, and E. Klavins, "Setpoint regulation for stochastically interacting robots," in *Proceedings of Robotics: Science and Systems*, Seattle, WA, USA, June 2009.

[12] N. Correll, "Parameter estimation and optimal control of swarm-robotic systems: A case study in distributed task allocation," in *Int'l. Conf. Robotics and Automation (ICRA)*, 2008, pp. 3302–3307.

[13] W. Liu and A. F. T. Winfield, "Modeling and optimization of adaptive foraging in swarm robotic systems," *Int'l. J. of Robotics Research*, vol. 29, no. 14, pp. 1743–1760, 2010.

[14] S. Berman, Á. Halász, M. A. Hsieh, and V. Kumar, "Optimized stochastic policies for task allocation in swarms of robots," *IEEE Trans. Robot.*, vol. 25, no. 4, pp. 927–937, August 2009.

[15] T. W. Mather and M. A. Hsieh., "Distributed robot ensemble control for deployment to multiple sites." *In Proceedings of Robotics: Science and Systems, LosAngeles, CA, USA*, 2011.

[16] A. Martinoli, K. Easton, and W. Agassounon, "Modeling swarm robotic systems: A case study in collaborative distributed manipulation," *Int'l. Journal of Robotics Research*, vol. 23, pp. 415–436, 2004.

[17] T. H. Labella, M. Dorigo, and J.-L. Deneubourg, "Division of labor in a group of robots inspired by ants' foraging behavior," *ACM Trans. Auton. Adapt. Syst.*, vol. 1, no. 1, pp. 4–25, 2006.

[18] N. Correll and A. Martinoli, "Modeling and optimization of a swarm-intelligent inspection system," in *Distributed Autonomous Robotic Systems 6*. Springer, 2007, pp. 369–378.

[19] T. P. Pavlic, S. Wilson, G. P. Kumar, and S. Berman, "An enzyme-inspired approach to stochastic allocation of robotic swarms around boundaries," in *Int'l. Symposium on Robotics Research (ISRR)*, Singapore, 2013.

[20] J. van Lint and R. Wilson, *A Course in Combinatorics*. New York, NY, USA: Cambridge University Press, 2001.

[21] H. David and H. Nagaraja, *Order Statistics*. Hoboken,NJ, USA: John Wiley and Sons, 2003.

[22] K. Murphy, *Machine Learning: A Probabilistic Perspective*. Cambridge,MA,USA: The MIT Press, 2012.

[23] K. Williams and J. Burdick, "Multi-robot boundary coverage with plan revision," in *Robotics and Automation, 2006. ICRA 2006. Proceedings 2006 IEEE International Conference on*, 2006, pp. 1716–1723.

[24] R. Motwani and P. Raghavan, *Randomized Algorithms*. New York, NY, USA: Cambridge University Press, 1995.

[25] G. P. Kumar, A. Buffin, T. P. Pavlic, S. C. Pratt, and S. M. Berman, "A stochastic hybrid system model of collective transport in the desert ant Aphaenogaster cockerelli," in *Proc. 16th Int'l. Conf. on Hybrid Systems: Computation and Control*, ser. HSCC'13, 2013, pp. 119–124.